03,13

Diffusion of Phosphorus and Gallium from a Deposited Layer of Gallium Phosphide into Silicon

© N.F. Zikrillaev[1], S.V. Koveshnikov[1], Kh.S. Turekeev[1,¶], N. Norqulov[2], S.A. Tachilin[1]

[1] Tashkent State Technical University,
Tashkent, Uzbekistan
[2] Mirzo Ulug'bek National University of Uzbekistan,
Tashkent, Uzbekistan

¶ E-mail: axmet-8686@mail.ru

Received April 27, 2022
Revised July 4, 2022
Accepted July 4, 2022

Diffusion from a layer of gallium phosphide GaP deposited onto a silicon surface was studied. After diffusion, the silicon samples were examined by the Van der Pauw method, and a scanning electron microscope was used to determine the concentration distribution of phosphorus and gallium atoms impurity.

Keywords: diffusion, gallium phosphide, silicon, solubility, concentration, binary complexes.

DOI: 10.21883/PSS.2022.11.54183.367

1. Introduction

An interesting field in the semiconductor physics is the creation of binary complexes in the crystal lattice of semiconductor materials [1–4], first of all, silicon. It is known that elements of groups III and V have a high solubility in silicon, but their diffusion coefficient has relatively small values, which hinders the formation of quasi-molecular compounds (complexes) in silicon lattice sites [5–8].

The aim of the present paper is to study the interaction of gallium and phosphorus atoms in the silicon lattice, which takes place during diffusion from a deposited layer of gallium phosphide GaP.

2. Experimental part

The initial material was single-crystal silicon Si (KDB-10) with the concentration of doping boron atoms $N_B \approx 2 \cdot 10^{15}\,\mathrm{cm}^{-3}$. A layer of GaP was deposited on the samples to study the diffusion process.

GaP in the form of powder with the grain size of $200-300\,\mu$m, obtained by crushing of single-crystal gallium phosphide FGECh-1-17, was used for deposition. A GaP layer $\sim 1\,\mu$m thick was deposited on silicon by vacuum thermal evaporation of the powder in the DILB832 unit using a silica boat and a tungsten heater. The heater was placed on the boat bottom and filled with GaP powder. The GaP powder evaporates during heating, is deposited on the Si-substrate, and settles on the silica boat internal surface. With further heating, the silica boat surface temperature rises, and GaP starts evaporating from the boat surface. Partial decomposition of GaP takes place in the boat surface during material redeposition, which manifests itself in a noticeable darkening of the film which covers the boat. The process of GaP deposition on the substrate was stopped by a damper when noticeable redeposition began. In this case, the deposited GaP film has the yellow color which is typical for the pure GaP material, and a high transparency to visible light. Diffusion from the deposited GaP layer was performed at $T = 1000^\circ$C for $t = 10$ h in vacuumized quartz ampoules. Diffusion of metal gallium into silicon and diffusion of phosphorus from ammonium phosphate in air was performed in separate ampoules in the same furnace. The samples doped only with gallium and only with phosphorus were used as references and allowed for studying the concentration distribution of these impurities in silicon along the depth. After diffusion, the sample surface was cleaned from possible residual contamination with diffusants and from phosphor-silicate glass using solutions — first 30% HCl, and then 10% HF. 3 groups of samples were obtained in this way.

Group I — samples doped from the GaP film. Group II — reference samples doped only with phosphorus. Group III — reference samples doped only with gallium.

Distribution of resistivity along the silicon sample depth was studied by mechanical layer-by-layer removal (polishing by $1\,\mu$m) and measurement of surface resistance and mobility using the van der Pauw method in the Van der Pauw Ecopia HMS-3000 unit.

3. Research results

The silicon samples with the deposited GaP layer were studied using a JSM-IT200 scanning election microscope (SEM) (electron beam energy — 20 keV) to determine the morphology and composition of the film (electron probe microanalysis) [9] on the silicon surface (Fig. 1 and Table 1).

The GaP film thickness for this sample did not exceed $1\,\mu$m, which is significantly less than the escape

Table 1. Composition of GaP film on silicon (the composition was determined using K-lines of elements)

Element	Mass, %	Atom, %
Si	90.62 ± 0.23	94.12 ± 0.24
P	3.74 ± 0.08	3.52 ± 0.07
Ga	5.65 ± 0.18	2.36 ± 0.08

depth of X-ray quanta of K-lines both in silicon (about 2000 nm) and in GaP (about 1400 nm). Therefore we can assume that the ratio of phosphorus and gallium concentrations was measured rather accurately, though their absolute concentrations have underestimated values. Considering the available average deviations of the atomic concentrations of gallium (8%) and phosphorus (7%), we can estimate the most probable phosphorus to gallium ratio — 1.49 : 1, i.e. a layer with phosphorus excess, as compared to the stoichiometric composition of GaP, forms after GaP deposition on the silicon surface.

The phosphorus excess is explained by the fact that GaP partially decomposes during deposition, and the resulting metal gallium virtually does not evaporate due to a low vapor pressure and remains in the boat. The presence of silicon in the results of the GaP film analysis is explained as follows: its thickness is less than the average track length of SEM electrons (for the energy of 20 keV in gallium phosphide it is $\sim 1.4\,\mu$m), that's why the spectrum has lines of silicon atoms pertaining to the Si-substrate. In this respect, it can be assumed that the film consists of a mixture of GaP and phosphorus. In the diffusion conditions ($T = 1000^\circ$C), the phosphorus excess quickly evaporates into the ampoule space, while the remaining film remains solid for some time (the melting temperature of gallium phosphide is $T = 1467^\circ$C).

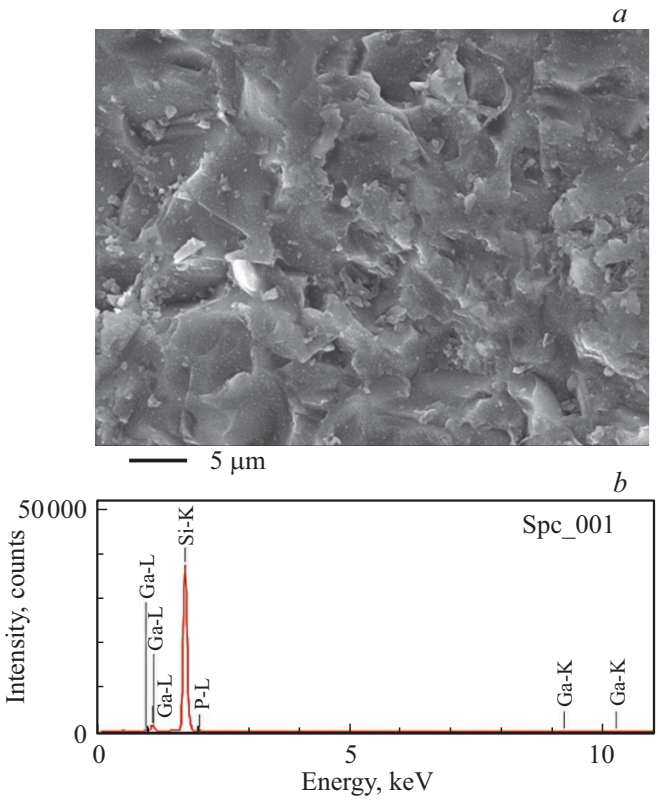

Figure 1. Morphology of gallium phosphide film on silicon.

This layer is a source for diffusion of gallium and phosphorus atoms into silicon; this ensures a high surface concentration of phosphorus and gallium (about $2.5 \cdot 10^{22}$ cm^{-3} in the beginning of the process). The film evaporates during diffusion (the equilibrium pressure of GaP vapor at $T = 1000^\circ$C is $P \approx 50$ mm Hg) and partially decomposes due to phosphorus evaporation into the ampoule space. According to [10], GaP evaporation in vacuum at temperatures below $T = 800^\circ$C is mainly congruent, while at higher temperatures GaP starts decomposing with the formation of phosphorus solution in metal gallium. Considering the diffusion temperature $T = 1000^\circ$C, as well as the low pressure of gallium vapors at this temperature ($P \approx 1$ mm Hg) [11], we can assume that phosphorus evaporates completely with the formation of vapor of phosphorus molecules [12]. Phosphorus concentration in the quartz ampoule, estimated according to film weight and ampoule volume, is not less than $\sim 10^{18}$ cm^{-3}. Solubility of phosphorus and gallium impurities at the diffusion temperature is equal to $N_P = 1 \cdot 10^{21}$ cm^{-3} and $N_{Ga} = 3 \cdot 10^{19}$ cm^{-3} respectively. This makes it possible to assume that diffusion of phosphorus atoms during diffusion from the film occurs both from the source with a concentration of at least $\sim 10^{18}$ cm^{-3}, while diffusion of gallium — as from a constant source (a metal gallium film on the silicon surface) with the concentration of $\sim 3 \cdot 10^{19}$ cm^{-3}.

In case of phosphorus diffusion in air, the following correlations can be used to determine the diffusion coefficient and impurity concentration:

$$D_P = 10.5 \cdot \exp\left(-\frac{3.66}{kT}\right);$$

$$N_P(x) = 1 \cdot 10^{21} \cdot \exp\left(-\frac{x^2}{4D_P t}\right),$$

at $T = 1000^\circ$C, $D_P = 3.5 \cdot 10^{-14}$ cm^2/s.

The following correlations can be used for the case of gallium diffusion in an evacuated quartz ampoule

$$D_{Ga} = 3.6 \cdot \exp\left(-\frac{3.49}{kT}\right);$$

$$N_{Ga}(x) = 4 \cdot 10^{19} \cdot \exp\left(-\frac{x^2}{4D_{Ga} t}\right),$$

at $T = 1000^\circ$C, $D_{Ga} = 5.6 \cdot 10^{-14}$ cm^2/s.

The concentration of gallium atoms changes during diffusion from the film. Under long-time diffusion, the gallium film oxidizes due to residual oxygen in the

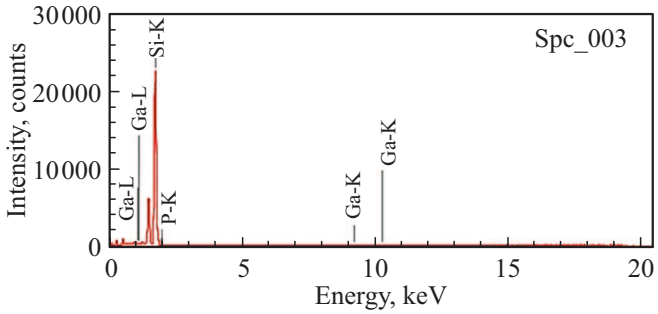

Figure 2. Composition of silicon surface layer after gallium phosphide diffusion from the deposited layer.

ampoule and oxygen from the silicone dioxide which covers the silicon, thus forming the gallium suboxide. The equilibrium pressure of Ga_2O vapors at the diffusion temperature is $P \approx 8$ mm Hg [13], which corresponds to $N_{Ga_2O} \approx 1 \cdot 10^{18}$ cm^{-3}.

The composition of the surface layer after GaP diffusion (Fig. 2 and Table 2) was also studied using a JSM-IT200 scanning election microscope.

The CASINO Monte Carlo Simulation software was used to calculate the escape depth and radial distribution of X-ray quanta in the material composed of 96% of silicon, 2% of gallium and 2% of phosphorus (Fig. 3).

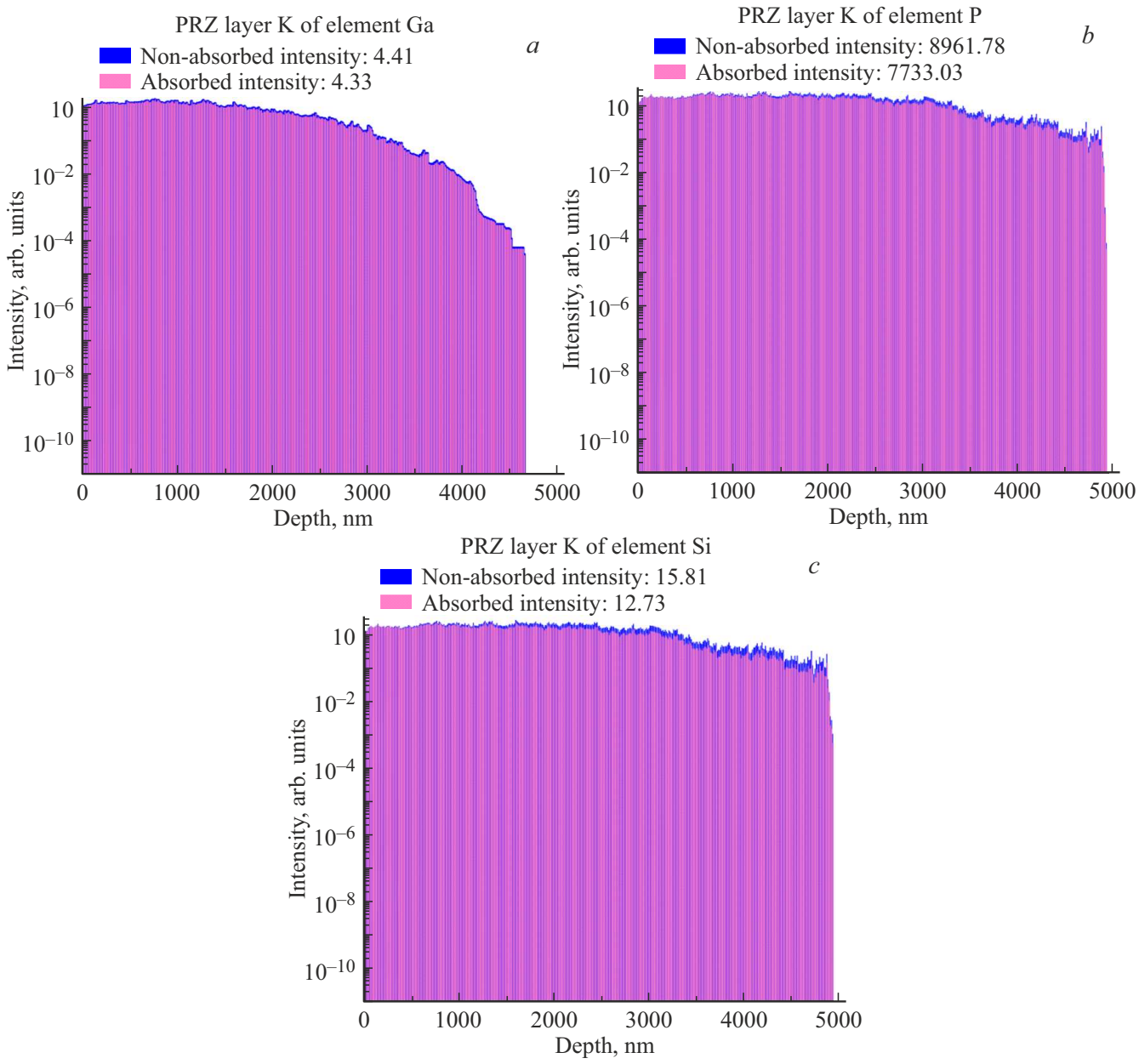

Figure 3. Dependence of intensity of K-lines of gallium (a), phosphorus (b), silicon (c) on escape depth, obtained using the CASINO Monte Carlo Simulation software.

Table 2. Composition of silicon surface layer after GaP diffusion from the deposited layer

Element	Mass, %	Atom, %
Si	97.52 ± 0.32	98.29 ± 0.33
P	1.39 ± 0.08	1.27 ± 0.07
Ga	1.10 ± 0.14	0.45 ± 0.06

This data shows that the escape depth of 75% of the X-ray quanta for the gallium K-line is $2\,\mu$m (the maximum at 900 nm), for the phosphorus K-line — $2.8\,\mu$m (the maximum at 1200 nm), for the silicon K-line — $2.7\,\mu$m (the maximum at 1200 nm). The escape radius of 75% of the X-ray quanta (taking into account the absorption) for the gallium, phosphorus and silicon K-lines is 150 nm. The identical value of the effective escape radius of the X-ray quanta is due to the low concentrations of gallium and phosphorus impurities, and the processes of transverse electron scattering are determined by the properties of the matrix — silicon. Given that the depths of the escape maxima for all the sample elements are close, it can be assumed that the composition data obtained using the JSM-IT200 SEM is an averaging over the volume in the shape of a cylinder having the height of 2800 nm and diameter of 300 nm.

Measurements were performed on the sample chip surface in order to increase the accuracy of the plotted phosphorus and gallium impurity concentrations. In this case, the depth resolving power of the method is estimated as 300 nm, and interpretation of the results is considerably simplified. Fig. 4 and Table 3 give some composition data obtained on the sample chip.

Fig. 5 gives the concentration distribution of gallium and phosphorus impurities plotted according to the results of measurements using the JSM-IT200 SEM on the sample chip.

The concentration measurement results obtained on the sample chip need a correction. The escape of X-ray quanta is higher (up to 2 times) in case of near-surface measurements, therefore, the impurity concentrations obtained from spectrum 011 are overestimated. On the other hand, averaging of the results by an area sized ~ 300 nm will cause smoothing of the doping profile. However, these phenomena do not hinder the measurement of the phosphorus to gallium concentration ratio. This ratio is equal to 3.21 : 1 for spectrum 011, to 3.57 : 1 for spectrum 012. These values show a significant change of solubility of these impurities in the conditions of joint diffusion. When the tabular values of phosphorus and gallium solubility in silicon is used, their ratio is $N_P/N_{Ga} = 1 \cdot 10^{21}/3 \cdot 10^{19} \approx 33$.

At the same time, the profile of phosphorus atom concentration (curve *3*) qualitatively matches the experimental profiles obtained in paper [14]. This means a predominant increase of gallium solubility.

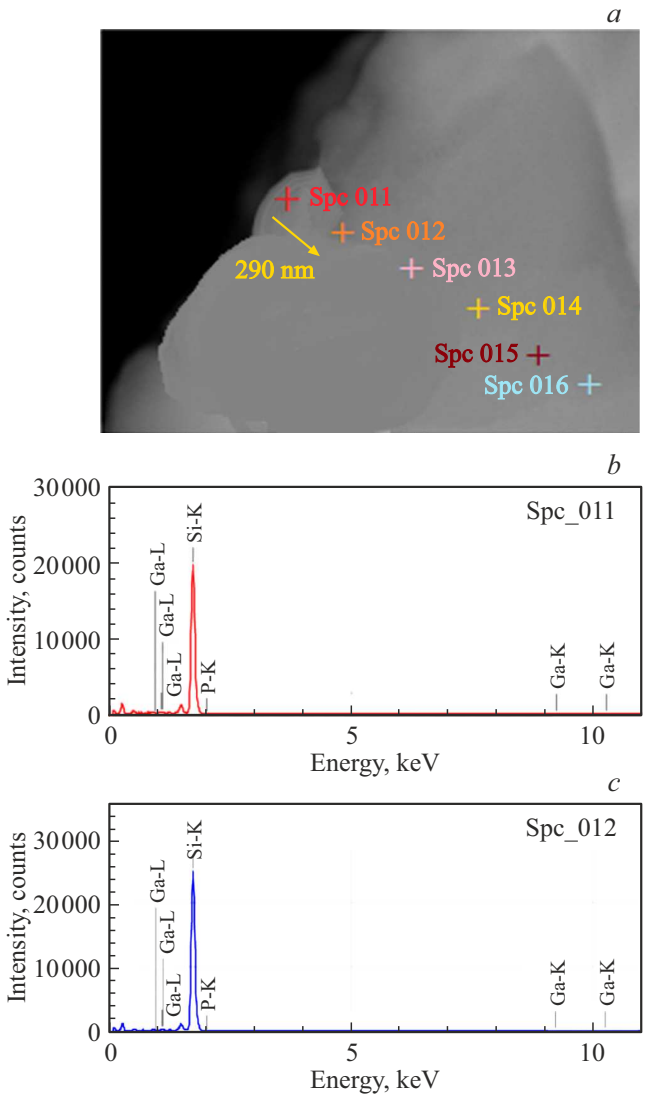

Figure 4. Composition data obtained on the sample chip: *a* — overall view of the chip butt, *b* — near the front surface (spectrum 011), *c* — at the depth of ~ 290 nm (spectrum 012).

Fig. 6 shows the experimental (the van der Pauw method) averaged distributions of charge carrier concentration along the depth in the silicon samples: reference group II — diffusion of phosphorus only, reference group III — diffusion of gallium only and group I — after diffusion from the deposited gallium phosphide layer.

The profile of charge carrier concentration was obtained by a calculation from the conductivity profiles. If an impurity is considered to be fully ionized, this profile matches the impurity concentration profile.

The experimental and estimated profiles of gallium atom distribution in reference group III matching within the 5% error.

After diffusion of phosphorus atoms only (reference group II), a layer of the *n*-type of conduction formed in silicon, and $p-n$-junction depth was $\sim 3\,\mu$m (curve *1*).

Table 3. Composition data obtained on the sample chip — near the front surface (spectrum 011) and at the depth of 290 nm (spectrum 012)

Element	Near the front surface (spectrum 011)		At the depth of ~ 290 nm (spectrum 012)	
	Mass, %	Atom, %	Mass, %	Atom, %
Si	96.71 ± 0.34	97.68 ± 0.35	98.65 ± 0.31	99.03 ± 0.31
P	1.93 ± 0.09	1.77 ± 0.09	0.83 ± 0.06	0.75 ± 0.06
Ga	1.36 ± 0.14	0.55 ± 0.06	0.52 ± 0.10	0.21 ± 0.04

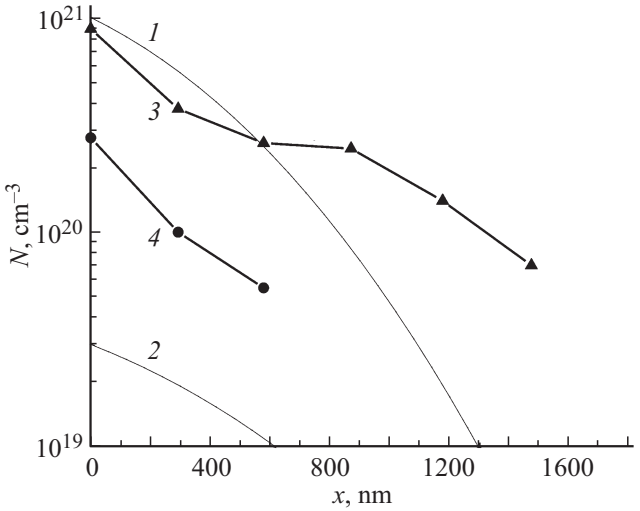

Figure 5. Distribution of phosphorus and gallium atom concentration in the silicon sample, doped from the gallium phosphide film, obtained on the sample chip using the JSM-IT200 SEM. Curve *1* — theoretical calculation of the phosphorus diffusion process, curve *2* — theoretical calculation of the gallium diffusion process, curve *3* — phosphorus, curve *4* — gallium.

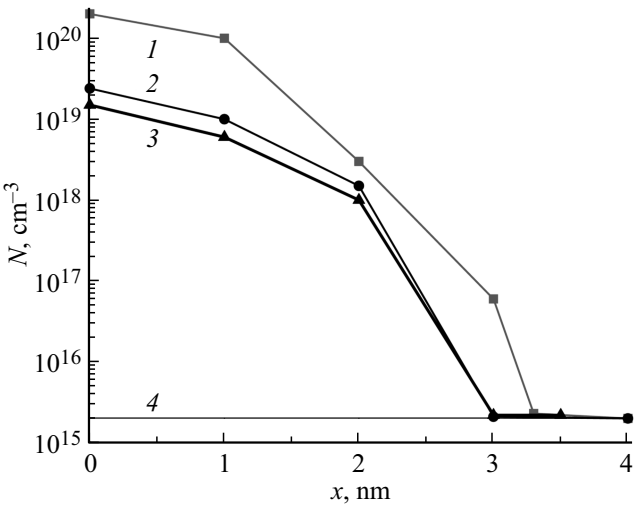

Figure 6. Experimental averaged distributions of charge carrier concentration along the depth in the silicon samples: curve *1* — reference group II (only phosphorus), curve *2* — reference group III (only gallium), curve *3* — group I (after diffusion from the deposited gallium phosphide layer) and boron concentration in the initial silicon (curve *4*).

The surface concentration of charge carriers calculated from the conductivity profiles [14] is $N_P = 2 \cdot 10^{20}$ cm^{-3}. These results agree well (within the 5% error) with the calculation of the diffusion profile of the phosphorus atom distribution in silicon according to the above-mentioned correlations, taking into account the experimentally obtained $p-n$-junction depth.

The phosphorus concentration for the samples of group I in the near-surface region, taking into account the compensation of phosphorus by gallium, can be estimated as a doubled concentration of gallium (curves *1* and *2*). This phosphorus concentration is almost 8 times lower than in the case of diffusion of only phosphorus into silicon (curve *6*). This, apparently, means that a significant part of phosphorus atoms passes to an electrically inactive state, due to the formation of phosphorus–gallium or phosphorus–phosphorus–gallium complexes.

4. Discussion of results

The analysis of the obtained results shows that a thin layer, consisting mainly of phosphorus and gallium atoms in the 1.5 : 1 ratio, forms after GaP thermal vacuum deposition on silicon. This is related to partial GaP decomposition during thermal deposition and low gallium volatility in the deposition conditions.

The measurements on the sample chip (obtained by diffusion from the GaP film) shows that the phosphorus to gallium concentration ratio reaches 3.21 : 1–3.57 : 1 in the sample's near-surface region. This is approximately by an order greater than the ration of the individual solubilities of these elements in silicon — 33 : 1. Given that the profile of phosphorus atom concentration qualitatively matches the experimental profiles obtained in [14], a predominant increase of gallium solubility can be assumed.

The results of measurements of the electroactive part of phosphorus and gallium concentrations (Fig. 6) for the same samples can be used to estimate the electroactive concentration of phosphorus as a doubled electroactive concentration of gallium (curves *1* and *2*). This phosphorus concentration is almost 8 times lower than in the case of diffusion of only phosphorus into silicon (curve *3*). These results cannot be explained only by the compensation of electroactive phosphorus atoms by electroactive gallium

atoms, since the fundamental value of gallium solubility is only $\sim 3\%$ from phosphorus solubility.

All this data, apparently, means that a significant part of phosphorus atoms passes to an electrically inactive state — possibly, due to the formation of phosphorus–gallium or other complexes.

The same samples are characterized by a significant increase of gallium solubility, as compared to its fundamental solubility. Such an increase can be also explained by the formation of gallium–gallium and gallium–phosphorus complexes. Similarly to [14], a highly doped by electrically inactive surface region is observed here, with a phosphorus concentration up to $\sim 10^{21}\,\mathrm{cm}^{-3}$, which causes a local increase of the diffusion coefficient in the near-surface region due to an increased lattice defectiveness. A significant change of the phosphorus diffusion coefficient with a concentration increase in the region of more than $\sim 10^{20}\,\mathrm{cm}^{-3}$ is also described in paper [15].

This phenomenon leads to the formation of a „horizontal" area on the phosphorus distribution profile [14] and an overall increase of its diffusion depth, which can be seen well in Fig. 5.

The distribution of gallium atom concentration (Fig. 5, curve *4*) also does not match the theoretical distribution (the experimental concentration of gallium atoms is considerably higher than the theoretical one), and there is also a slight decrease of the diffusion coefficient. This can be explained by the process of complex formation between gallium and phosphorus atoms, which is rather efficient in the region of the high phosphorus concentration. Gallium and phosphorus atoms can occupy voids in divacancies, the concentration of which in the near-surface region highly doped with phosphorus is high [16]. An estimation of the Coulombic energy of the gallium–phosphorus bond in the silicon lattice yields a value of about $\sim 0.5\,\mathrm{eV}$. In equilibrium conditions, according to the Arrhenius correlation, this can cause an increase of gallium concentration up to ~ 10 times, which matches the obtained experimental results.

The numerical calculations show that the gallium and phosphorus bond energy has the same order as the bond energy of vacancies in divacancies. It can be assumed that the equilibrium concentration of divacancies is equal to the equilibrium concentration of gallium–phosphorus complexes. The concentration of divacancies at the diffusion temperature is estimated as $\sim 10^{20}\,\mathrm{cm}^{-3}$ [17], which also makes it possible to estimate the concentration limit of gallium–phosphorus complexes.

The formation of divacancies and their filling with impurities makes it possible to assume that gallium–gallium and phosphorus–phosphorus complexes originate during the diffusion. It is difficult to estimate the bond energy of such complexes in the silicon lattice. The estimated bond energy for phosphorus complexes is equal to $\sim 0.85\,\mathrm{eV}$ [3]. The value of $\sim 0.45\,\mathrm{eV}$ was obtained for gallium–gallium complexes, taking into account the possible metallic bond. This bound energy virtually coincides with the estimated phosphorus–gallium bond energy. Both effects of gallium

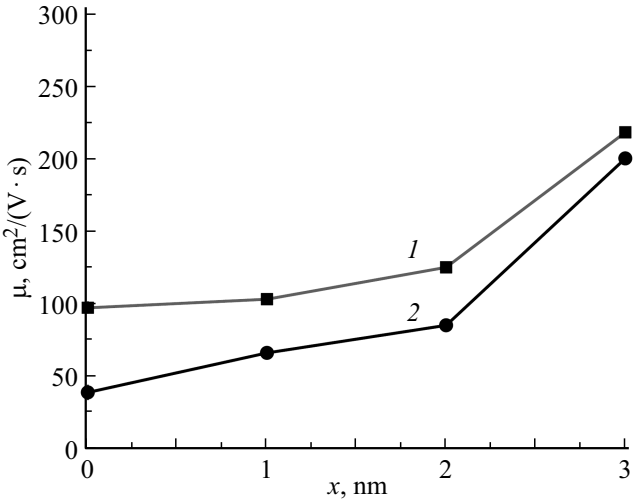

Figure 7. Electron mobility in silicon doped with only impurity atoms of phosphorus (curve *1*) and doped from the deposited gallium phosphide layer (curve *2*).

complex formation may cause an increase of gallium solubility. Taking this into account, we can estimate the maximum gallium concentration in the silicon lattice as a value of the order of divacancy concentration $\sim 10^{20}\,\mathrm{cm}^{-3}$.

Moreover, the solubility of gallium atoms in silicon can increase due to a slight change of the silicon lattice constant in case of heavy doping with phosphorus. It is difficult to estimate such a solubility increase.

Profiles of charge carrier mobilities were plotted in order to estimate the possible influence of complex formation on samples' properties.

Fig. 7 shows the profiles of charge carrier mobilities along the depth for the obtained silicon samples, determined by the van der Pauw method.

It is known from literature [18] that when electron concentration in silicon is equal to $N \approx 10^{19}-10^{20}\,\mathrm{cm}^{-3}$, their mobility must be $\mu \approx 80-90\,\mathrm{cm}^2/(\mathrm{V}\cdot\mathrm{s})$.

As can be seen from Fig. 7, the silicon samples, doped only with phosphorus atoms and doped from the deposited GaP layer, have the *n*-type of conduction up to the depth of $3\,\mu$m. However, electron mobility in the layer doped from the gallium phosphide film is up to three times smaller than electron mobility in the layer doped only with phosphorus atoms.

It can be assumed that such a considerably mobility decrease is related to the presence of an electroactive part of gallium atoms, which is comparable (about half the electroactive concentration of phosphorus, according to Fig. 6, curves *1* and *2*) with the value of ionized phosphorus concentration, as well as an increase of scattering due to the influence of electroneutral complexes.

The complexes have a large share of the ionic bond, that's why the scattering properties of Ga and P ions, which make up electroneutral complexes, are comparable to the scattering properties of Ga and P ions separately.

Moreover, the mobility decrease can be related to a change of charge carrier scattering on lattice heterogeneities (multicomplexes of the $(GaP)_n$ type in the silicon lattice) near-surface concentration of which can be rather high. As seen in Fig. 4, the total concentration of donor and acceptor impurities in the near-surface layer in case of simultaneous diffusion can exceed the solubility limit of each impurity separately. The increase of solubility of donor and acceptor impurities correlates with the additional decrease of mobility. Thus, a decrease of mobility can be considered dependent only on solubility of impurities, regardless of whether they form electroneutral binary complexes or simply compensate each other. We believe that a threefold decrease of mobility as compared to the theoretical values means an at least threefold increase of phosphorus and gallium solubility in case of their simultaneous diffusion.

5. Conclusion

There are significant deviations both of electroactive and total solubility of phosphorus and gallium impurities in case of their simultaneous diffusion from gallium phosphide layers into silicon. Changes in phosphorus and gallium behavior during diffusion from the gallium phosphide film can be explained by an interaction of gallium and phosphorus atoms with the formation of electroneutral complexes in silicon. An estimation of the Coulombic energy of the gallium–phosphorus bond in the silicon lattice yields a value of about ~ 0.5 eV. The estimated bond energy for phosphorus complexes is equal to ~ 0.85 eV [3]. The value of ~ 0.45 eV was obtained for gallium–gallium complexes, taking into account the possible metallic bond. Effects of gallium complex formation may result in an increase of gallium solubility to a value of the order of divacancy concentration in silicon at the diffusion temperature ($T = 1000^\circ$C) $\sim 10^{20}$ cm^{-3}. The revealed threefold decrease of mobility in the obtained samples as compared to the theoretical values means a significant increase of phosphorus and gallium solubility in case of their simultaneous diffusion.

Gallium–phosphorus binary complexes, forming in rather large concentrations, can significantly affect the electrophysical, optical and photovoltaic properties of silicon. Estimation of this influence requires an integrated study of materials having rather a high concentration of molecular complexes such as $Si_2Ga^-P^+$ in the silicon lattice [19,20].

Funding

The research was conducted within the framework of scientific project-54 (fundamental project) 21101836.

Conflict of interest

The authors declare that they have no conflict of interest.

References

[1] M.K. Bakhadyrkhanov, S.B. Isamov. ZhTF **91**, *1*, 1678 (2021) (in Russian).
[2] M.K. Bakhadyrkhanov, N.F. Zikrillaev, S.B. Isamov, Kh.S. Turekeev, S.A. Valiev. FTP **56**, *2*, 199 (2022) (in Russian).
[3] M.K. Bakhadyrkhanov, Z.T. Kenzhaev, S.V. Koveshnikov, A.A. Usmonov, G.Kh. Mavlonov. Neorgan. materialy **58**, *1*, 3 (2022) (in Russian).
[4] K.A. Ismaylov, Z.T. Kenzhaev, S.V. Koveshnikov, E.Zh. Kosbergenov, B.K. Ismaylov. FTT **64**, *5*, 519 (2022) (in Russian).
[5] M.K. Bakhadyrkhanov, Kh.M. Iliev, G.Kh. Mavlonov, K.S. Ayupov, S.B. Isamov, S.A. Tachilin. Tech. Phys. **64**, *3*, 385 (2019).
[6] M.K. Bakhadyrkhanov, S.B. Isamov, N.F. Zikrillaev, Kh.M. Iliev, G.Kh. Mavlonov, S.V. Koveshnikov, Sh.N. Ibodullaev. Elektronnaya obrabotka materialov **56**, *2*, 14 (2020) (in Russian).
[7] S. Adachi. Properties of group-IV, III-V and II-VI semiconductors. John Wiley and Sons Ltd (2005). 400 p.
[8] A.S. Saidov, D.V. Saparov, Sh.N. Usmonov, A. Kutlimuratov, J.M. Abdiev, M. Kalanov, A.Sh. Razzakov, A.M. Akhmedov. Adv. Condens. Matter Phys. Hindawi 2021. Article ID 3472487 (2021). https://doi.org/10.1155/2021/3472487
[9] G.M. Zeer, O.Yu. Fomenko, O.N. Ledyayeva. Zhurn. Sibir. federlanogo un-ta. Khimiya **4**, *2*, 287 (2009) (in Russian).
[10] D.V. Ryazanov. Avtoref. kand. diss. Vzaimodeistviya komponentov v fosfide galliya i ego rastvorakh v gallii. Voronezh. gos. tekhn. un-t. Voronezh(1998). 18 s. (in Russian).
[11] S.P. Yatsenko, L.A. Pasechnik, V.M. Skachkov, G.M. Rubinshtein. Galliy: tekhnologiya polucheniya i primeneniye zhidkikh splavov. Izd-vo RAN, M. (2020). 344 s. (in Russian). ISBN 978-5-907036-93-2
[12] R. Fornari, A. Brinciotti, A. Sentiri, T. Gorog, M. Curti, G. Zuccalli. J. Appl. Phys. **75**, *5*, 2406 (1994).
[13] E.K. Kazenas, D.M. Chizhikov. Davleniye i sostav para nad okislami khimicheskikh elementov. Nauka, M. (1976). 344 s. (in Russian).
[14] M.W. Hwang, M.Y. Um, Y-H. Kim, S.K. Lee, H.J. Kim, W.Y. Park. J. Korean Vacuum Sci. Technol. **4**, *3*, 73 (2000).
[15] E. Tannenbaum. Solid State Electronics **2**, *2–3*, 123 (1961). DOI: 10.1016/0038-1101(61)90029-6
[16] B.I. Boltaks. Diffuziya v poluprovodnikakh. Fizmatgiz, M. (1961). 462 s. (in Russian).
[17] I.I. Novikov. Defekty kristallicheskogo stroyeniya metallov. Metallurgiya, M. (1975). 207 s. (in Russian).
[18] G. Kaiblinger-Grujin, H. Kosina, S. Selberherr. J. Appl. Phys. **83**, *6*, 3096 (1998).
[19] M.K. Bakhadyrkhanov, U.X. Sodikov, Kh.M. Iliev, S.A. Tachilin, T. Wumaier. Mater. Phys. Chem. **1**, *1*, 8 (2019). DOI: 10.18282/mpc.v1i1.569
[20] M.K. Bakhadirkhanov, S.B. Isamov, Z.T. Kenzhaev. EuroAsian J. Semicond. Sci. Eng. **2**, *5*, 9 (2020).